UJRET
Bi-annual refereed journal
University Journal of Research Engineering & Technology
September 2024
Volume 1, (1) pp. 40-62

Investigation on Mechanical Properties of Material Extrusion Additive Manufactured Specimen using PVDF Feedstock Material

Trivedi Achyut
Chairperson, Centre of Excellence for Additive Manufacturing
Faculty of Engineering and Technology, Ganpat University, Gujarat, 384012, India

Hetal Vasava
Research Scholar, Department of Mechanical Engineering
Faculty of Engineering and Technology, Ganpat University, Gujarat, 384012, India

Abstract

Additive manufacturing, particularly fused deposition modeling (FDM), has gained significant traction due to its ability to rapidly prototype and fabricate complex geometries. However, achieving desired mechanical properties in FDM-printed parts remains a challenge, necessitating comprehensive exploration and optimization of printing parameters. This study systematically investigates the influence of nozzle temperature, bed temperature, layer thickness, and part orientation on the mechanical properties of FDM-printed parts using a factorial central composite design (FCCCD) approach. The results reveal the significant impact of printing parameters on both tensile and flexural strengths of printed parts. As nozzle temperature emerges as a critical factor, with higher temperatures generally leading to improved mechanical properties due to enhanced layer adhesion and interlayer bonding. Similarly, higher bed temperatures promote better interlayer adhesion and reduce warping or shrinkage stresses. Thinner layer thickness results in higher mechanical strengths due to finer resolution and improved interlayer bonding. Part orientation significantly affects mechanical properties, with vertically oriented parts exhibiting superior strengths compared to horizontally oriented parts, highlighting the anisotropic behavior of FDM-printed parts. By analyzing the experimental data and employing fuzzy logic analysis, this study facilitates the optimization of printing parameters to achieve desired mechanical properties in FDM-printed parts. These insights enable manufacturers to tailor the mechanical characteristics of printed components to meet specific application requirements, enhancing performance and reliability in industries such as aerospace, automotive, and medical sectors. The study's rigorous approach contributes to the advancement of additive manufacturing research methodologies and lays the foundation for future research and innovation in the field.

Keywords: PVDF, FDM, Additive Manufacturing, AM, Expert system in AM

1. Introduction

Additive manufacturing (AM), commonly known as 3D printing, is a revolutionary process that has transformed the landscape of manufacturing and design. Unlike traditional subtractive manufacturing, which involves

Corresponding author. Tel.:
E-mail address:atrivedi8866@gmail.com

cutting away material from a solid block, additive manufacturing builds objects layer by layer from the ground up. This method allows for unprecedented design flexibility, material efficiency, and the potential for customized production (Gibson et al., 2010). The origins of additive manufacturing can be traced back to the 1980s, with the advent of stereolithography (SLA), the first AM technology developed by Charles Hull. Since then, the field has evolved significantly, encompassing a wide range of techniques and materials. The key technologies include fused deposition modeling (FDM), selective laser sintering (SLS), and direct metal laser sintering (DMLS), among others. Each of these technologies uses different materials, from plastics and resins to metals and ceramics, allowing for a diverse array of applications (Gupta et al., 2017). One of the primary advantages of additive manufacturing is its ability to produce complex geometries that would be impossible or highly impractical with traditional manufacturing methods. This capability is particularly beneficial in industries such as aerospace, automotive, and healthcare, where intricate designs can lead to significant performance improvements. For instance, in the aerospace industry, AM is used to create lightweight components that reduce overall aircraft weight, thereby improving fuel efficiency and reducing emissions (Wohlers et al., 2014). Fused Deposition Modeling (FDM) is one of the most widely utilized techniques in additive manufacturing (AM). This technology has revolutionized the manufacturing sector by offering a cost-effective, efficient, and versatile method of producing complex geometries that traditional manufacturing processes struggle to achieve (Crump, 1992). FDM works by extruding thermoplastic filaments through a heated nozzle, layer by layer, to build a three-dimensional object from a digital model. This layer-by-layer approach enables the creation of parts with intricate internal structures and varying densities, catering to diverse industrial applications (Chua & Leong, 2017). FDM was invented by Scott Crump in the late 1980s and commercialized by Stratasys in the early 1990s. The technology's inception marked a significant milestone in the evolution of additive manufacturing, providing a new avenue for rapid prototyping and production. Over the years, advancements in material science and machine design have significantly enhanced the capabilities of FDM printers, making them more accessible to a broader range of users, from hobbyists to industrial manufacturers (Jones et al., 2011).

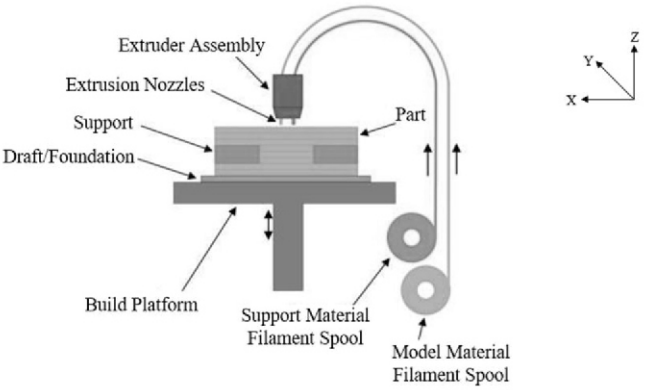


Figure 1 Schematic diagram of FDM process

One of the most significant areas of development in FDM is the enhancement of filament materials. Researchers have made considerable progress in developing composite filaments that incorporate carbon fibers, glass fibers, and metal particles to enhance mechanical properties and thermal performance (Tekinalp et al., 2014; Ning et al., 2015). For instance, studies have shown that carbon fiber-reinforced filaments exhibit improved tensile strength and stiffness compared to traditional thermoplastics (Tian et al., 2016; Compton et al., 2017). Similarly, the integration of metal particles into filaments has led to the creation of parts with higher thermal conductivity and structural integrity, suitable for more demanding applications (Duty et al., 2017). High-performance polymers such as polyether ether ketone (PEEK) and

polyetherimide (ULTEM) have also been explored extensively for their superior mechanical and thermal properties. These materials are particularly relevant in industries that require high strength and thermal resistance, such as aerospace and medical devices (Bikas et al., 2016). Research indicates that optimizing the processing parameters for these high-performance materials can further enhance their properties, making them viable for critical applications (Song et al., 2017). Optimizing FDM process parameters is crucial for improving the quality and performance of printed parts. Recent studies have focused on refining parameters such as layer thickness, printing speed, nozzle temperature, and infill density. For example, reducing layer thickness can enhance the surface finish and dimensional accuracy of printed parts, although it may increase the overall printing time (Cheng et al., 2016). Conversely, increasing the nozzle temperature can improve inter-layer adhesion but might lead to material degradation if not properly controlled (Ahn et al., 2002). Advanced algorithms and machine learning techniques are being employed to optimize these parameters dynamically. Researchers have developed predictive models that can adjust printing parameters in real-time based on feedback from the printing process, thereby improving print quality and reducing the incidence of defects (Ding et al., 2018; Baumann et al., 2019). Such innovations are paving the way for more reliable and efficient FDM processes. FDM technology has seen significant application-specific advancements, particularly in the aerospace, medical, and automotive industries. In aerospace, the focus has been on developing lightweight, high-strength components that can withstand extreme conditions. Studies have highlighted the use of PEEK and ULTEM for producing aircraft components due to their excellent mechanical properties and resistance to high temperatures (Hopkinson et al., 2006; Gardan et al., 2015). Additionally, researchers are exploring the use of FDM for manufacturing satellite components, where weight reduction is a critical factor (Goh et al., 2014). In the medical field, FDM has been instrumental in producing patient-specific implants, prosthetics, and anatomical models. Recent research has demonstrated the effectiveness of using biodegradable and bioresorbable materials for medical applications, which can safely degrade within the body after fulfilling their function (Bose et al., 2013). Innovations such as multi-material printing are also being explored to create more complex medical devices with varying properties in different regions of the part (Hollister, 2005; Murphy & Atala, 2014). The automotive industry continues to benefit from FDM's rapid prototyping capabilities, which allow for quick iteration and testing of new designs. Recent advancements include the development of more durable and heat-resistant materials for under-the-hood applications, as well as the use of FDM for producing jigs, fixtures, and end-use parts (Turner et al., 2014; Gao et al., 2015). These innovations are helping manufacturers reduce lead times and costs associated with traditional manufacturing methods. Despite the progress, FDM still faces several challenges that need to be addressed. One of the main issues is the anisotropic nature of printed parts, where mechanical properties differ along different axes due to the layer-by-layer deposition process. This anisotropy can lead to weaker inter-layer bonding and reduced overall strength (Es-Said et al., 2000; Rodriguez et al., 2001). Research is ongoing to develop new materials and printing techniques that can mitigate this issue, such as using high-performance adhesives or incorporating post-processing steps like annealing (Farahani & Dube, 2017).

Polyvinylidene fluoride (PVDF) is emerging as a promising material in the realm of FDM due to its unique properties. PVDF is a semi-crystalline thermoplastic known for its high chemical resistance, mechanical strength, and excellent thermal stability. Its potential to fill the gap and address some of the key challenges in FDM is notable for several reasons. PVDF exhibits superior inter-layer bonding compared to many conventional FDM materials. Its inherent material properties contribute to enhanced layer adhesion, which can significantly reduce the anisotropic weakness commonly observed in FDM parts (Liu et al., 2018). Research indicates that PVDF's crystalline structure and thermal properties help achieve better fusion between layers, leading to improved mechanical strength and durability (Zhang et al., 2018). One of the standout features of PVDF is its excellent resistance to a wide range of chemicals, including acids, bases, and solvents. This makes PVDF an ideal candidate for applications in harsh chemical environments where traditional FDM materials would degrade. Utilizing PVDF in FDM can

expand the scope of applications, particularly in the chemical processing and medical industries, where chemical resistance is paramount (Wang et al., 2019). PVDF's high thermal stability allows it to maintain structural integrity at elevated temperatures. This property is particularly beneficial for applications requiring parts that can withstand high-temperature conditions without deforming. Incorporating PVDF in FDM can lead to the production of components that are both thermally stable and mechanically robust, addressing a critical limitation of many standard FDM materials (Huang et al., 2018). PVDF is amenable to various post-processing techniques that can further enhance its properties. For instance, annealing PVDF parts can improve their crystallinity and mechanical performance. Additionally, PVDF's surface can be functionalized to enhance its compatibility with other materials or to impart specific surface properties, such as hydrophobicity or conductivity. These capabilities make PVDF a versatile material for advanced FDM applications (Li et al., 2019; Zhao et al., 2020). PVDF is also known for its excellent piezoelectric and dielectric properties. This makes it suitable for electronic and sensor applications where materials need to exhibit specific electrical behaviors. Using PVDF in FDM can open up new possibilities in the production of electronic components, sensors, and actuators directly through additive manufacturing processes (Sencadas et al., 2012).

2. Materials and Methods

2.1 Polyvinylidene fluoride (PVDF)

Polyvinylidene fluoride (PVDF) is gaining traction as a promising feedstock material for Fused Deposition Modeling (FDM) due to its exceptional properties, which include high chemical resistance, excellent thermal stability, and good mechanical strength. Figure 2 shows chemical structure of PVDF. PVDF is a semi-crystalline polymer known for its durability and robustness in harsh environments, making it suitable for applications in various industries such as chemical processing, aerospace, and electronics.

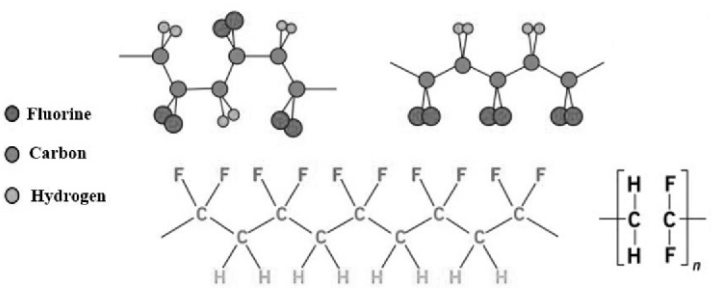


Figure 2. Material Composition of PVDF [34]

Table 1 shows the material PVDF properties. One of the primary advantages of using PVDF in FDM is its high chemical resistance, which allows it to withstand exposure to a wide range of chemicals, including acids, bases, and organic solvents. candidate for producing components that This property makes PVDF an ideal require long-term exposure to corrosive environments. Additionally, PVDF's thermal stability enables it to maintain its mechanical properties at elevated temperatures, thereby expanding the range of applications for FDM-printed parts.

Table 1. PVDF Material Properties

Material Property	Value
Chemical Resistance	Excellent
Thermal Stability	High
Melting Point	170°C to 175°C
Tensile Strength	40-50 MPa
Impact Resistance	Good
Wear Resistance	Good
Density	1.78 g/cm³
Dielectric Strength	16-20 kV/mm
UV Resistance	Excellent
Flexural Modulus	1.2-1.5 GPa
Elongation at Break	20-25%

2.2 Fabrication of samples using Design of Experiment approach

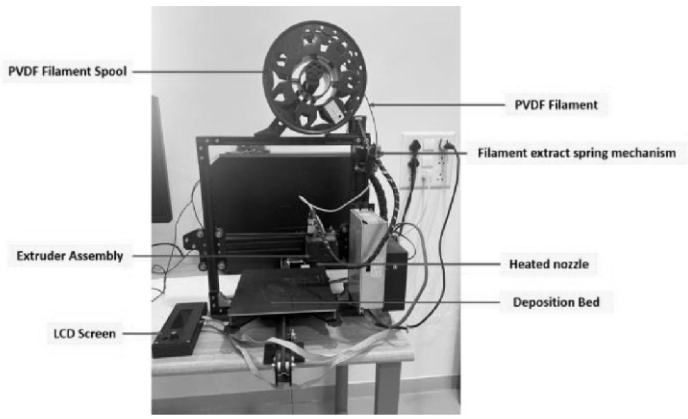


Figure 2. FDM base 3D Printer for part manufacturing using PVDF

The Face-Centered Central Composite Design (FCCCD) is a widely used method in the Design of Experiments (DoE) for optimizing processes with multiple variables. The FCCCD approach involves running experiments at all combinations of the factor levels, including the center points. This design not only allows for the estimation of linear and interaction effects but also quadratic effects, which are crucial for understanding the non-linear behavior of the process parameters. In the present work, Tevo Tarantula® 3D Printer is used to fabricate the specimens. Also, Figure 3 shows FDM base 3D Printer used in present work for part manufacturing using PVDF feedstock filament material. The Face-Centered Central Composite Design (FCCCD) is an effective DoE method for optimizing FDM process parameters. By systematically varying nozzle temperature, bed temperature, layer thickness, and part orientation, researchers can identify optimal conditions that enhance the quality and performance of 3D-printed parts. This approach not only improves the understanding of the FDM process but also contributes to more efficient and reliable additive manufacturing practices. In the present work of Fused Deposition Modeling (FDM), FCCCD helps in systematically studying the effects of key process parameters on the quality of printed parts. In the present work of Fused Deposition Modeling (FDM), FCCCD helps in systematically studying the effects of key process parameters on the quality of printed parts. The process parameters considered in FDM include nozzle temperature, bed temperature, layer thickness, and part orientation. The Table 2 shows FDM process parameters, their units, symbols, and levels used in the FCCCD design. Table 3 mentioned the schema for FCCCD design matrix.

2.3 Testing Methodologies

Table 2. Process parameters settings and their levels

Process Parameters	Units	Symbol	Levels		
			-1	0	+1
Nozzle Temperature	°C	A	200	215	230
Bed Temperature	°C	B	80	90	100
Layer Thickness	mm	C	0.1	0.18	0.35
Part Orientation	°	D	0	45	90

In the present work, ASTM D638 and ASTM D790 testing methods were employed to assess the mechanical properties of Fused Deposition Modeling (FDM) printed Polyvinylidene Fluoride (PVDF) material. ASTM D638 standards were utilized to determine the tensile properties of the printed PVDF specimens, including parameters such as tensile strength, elongation at break, and modulus of elasticity. Meanwhile, ASTM D790 guidelines were followed for flexural testing, allowing for the evaluation of flexural strength, flexural modulus, and deformation behavior under three-point bending conditions. By adhering to these standardized testing procedures, the study aimed to ensure consistency and reliability in characterizing the mechanical performance of FDM-printed PVDF material, providing valuable insights into its suitability for various engineering applications. Figure 4 and 5 represent detail drawing of Specimen as per ASTM D638 (type -I) and detail drawing of Specimen as per ASTM D790 respectively.

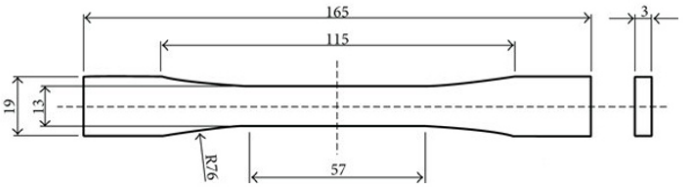


Figure 4. Detail drawing of Specimen as per ASTM D638 (type -I) (all dimensions are in mm)

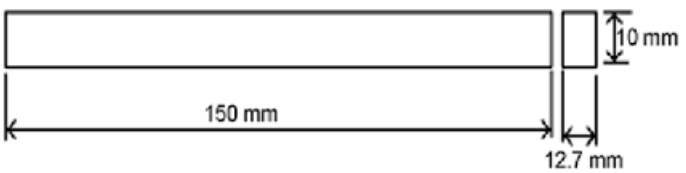


Figure 5. Detail drawing of Specimen as per ASTM D790 (all dimensions are in mm)

2.4 Fuzzy Logic System

Applying fuzzy logic involves several steps. First, linguistic variables representing the input and output parameters of the system are defined. For instance, tensile strength is the linguistic variable for ASTM D638 testing, and flexural strength is for ASTM D790 testing. Next, fuzzy set membership functions are established to denote the degree of membership of each linguistic variable in its respective fuzzy set.

Table 3. FCCCD Design Schema Matrix

Run	Nozzle Temperature (°C)	Bed Temperature (°C)	Layer Thickness (mm)	Part Orientation (°)
1	230	80	0.35	90
2	215	80	0.225	45
3	230	80	0.35	0
4	230	80	0.1	90
5	230	100	0.35	90
6	230	100	0.1	90
7	200	100	0.35	90
8	200	90	0.225	45
9	200	80	0.1	90
10	200	100	0.1	90
11	200	100	0.35	0
12	230	80	0.1	0
13	215	90	0.225	45
14	215	90	0.225	45
15	215	90	0.1	45
16	200	80	0.35	90
17	215	90	0.225	45
18	215	90	0.225	0
19	215	90	0.225	45
20	230	100	0.1	0
21	215	100	0.225	45
22	215	90	0.35	45
23	215	90	0.225	45
24	215	90	0.225	90
25	200	80	0.35	0
26	215	90	0.225	45
27	200	80	0.1	0
28	230	90	0.225	45
29	230	100	0.35	0
30	200	100	0.1	0

These functions can be triangular, trapezoidal, or Gaussian, depending on the desired shape. For example, the membership function for "high tensile strength" in ASTM D638 testing assigns higher values to specimens with greater tensile strength. The rule base construction follows, consisting of IF-THEN rules that encode expert knowledge or heuristics about the relationships between input and output variables. These rules guide the fuzzy inference process by capturing qualitative relationships. An example rule might be: "IF tensile strength is high AND elongation at break is low THEN material quality is good." The fuzzy inference process then combines the input variables, membership functions, and rule base to determine the degree of membership of each output variable. This involves fuzzification, where crisp input values are transformed into fuzzy sets, and inference, where the rules are applied to ascertain the degree of membership of each output variable. Defuzzification is the final step, where the fuzzy output values are converted back into crisp, numerical results. Various methods, such as centroid, maximum membership, or weighted average, can be used for defuzzification. Finally, the crisp output values are

interpreted and analyzed to draw conclusions about the mechanical properties of the material. This involves comparing the fuzzy logic-based results with conventional testing methods, identifying any discrepancies or insights, and refining the fuzzy logic model if necessary.

3. Results and Discussions

3.1 Results and Discussions on experimental works

The experimental results of the tensile strength obtained from the Face-Centered Central Composite Design (FCCCD) experiments are summarized in Table 4. The table presents the tensile strength values (in MPa) corresponding to each experimental run, along with the corresponding levels of the input factors, including nozzle temperature, bed temperature, layer thickness, and part orientation. The data indicate significant variability in tensile strength across different experimental conditions. Notably, runs with variations in the nozzle temperature, bed temperature, layer thickness, and part orientation yielded diverse tensile strength values, reflecting the sensitivity of the Fused Deposition Modeling (FDM) process to these parameters. Among the experimental runs, the highest tensile strength was observed in run 13, where the nozzle temperature was set at 215°C, bed temperature at 90°C, layer thickness at 0.225 mm, and part orientation at 45°, resulting in a tensile strength of 38.88 MPa. Conversely, run 18 exhibited the lowest tensile strength of 26.12 MPa, corresponding to a nozzle temperature of 215°C, bed temperature of 90°C, layer thickness of 0.225 mm, and part orientation of 0°. The experimental results presented in Table 4 serve as a valuable foundation for understanding the effects of process parameters on the tensile properties of FDM-printed PVDF material, contributing to the advancement of additive manufacturing technologies and material science research. Table 5 shows the Analysis of Variance (ANOVA) table for tensile strength. The ANOVA table provides a comprehensive summary of the analysis of variance for the experimental data, assessing the significance of the model and individual factors influencing the response variable, which is the tensile strength in this case. In this case, the model is highly significant ($p < 0.0001$), indicating that the variation in tensile strength can be explained by the chosen factors and their interactions. Each factor and interaction term are evaluated separately to determine their significance. Factors A, B, D, AD, and CD are found to be significant ($p < 0.05$), indicating that they have a significant impact on tensile strength. Factors C, AB, AC, BC, BD, and interactions A^2, B^2, C^2, and D^2 are not significant ($p > 0.05$), suggesting that they do not have a significant influence on the response. The residual sum of squares represents the unexplained variability in the model. The lack of fit test compares the variation within groups to the variation between groups. In this case, the lack of fit is not significant ($p = 0.4676$), indicating that the model adequately fits the data, and there is no significant discrepancy between the model predictions and observed data. The coefficient of determination (R-squared) measures the proportion of the total variation in the response variable explained by the model. In this case, the R-squared value is high (0.9833), indicating that the model explains approximately 98.33% of the variability in tensile strength. Adjusted R-squared and predicted R-squared values are also provided, which adjust for the number of predictors in the model.

Table 6 shows the Analysis of Variance (ANOVA) table for flexural strength. The model section assesses the overall significance of the regression model. The calculated F-value (16.36) indicates that the model is statistically significant (p-value < 0.0001), suggesting that at least one of the input factors (A, B, C, or D) significantly influences the response variable (tensile strength). This finding implies that the model is effective in explaining the variation in the response variable. These sections evaluate the significance of each individual factor (Nozzle Temperature, Bed Temperature, Layer Thickness, Part Orientation) in influencing the response variable. Among these factors, factor A (Nozzle Temperature) shows the highest significance, with an extremely low p-value (< 0.0001), indicating a highly significant effect on tensile strength. Conversely, factors B (Bed Temperature), C (Layer Thickness), and D (Part Orientation) exhibit higher p-values, suggesting relatively lower significance levels. However, it's important to note that even

though factor B, C, and D are not statistically significant at conventional significance levels ($p > 0.05$), they may still have practical significance or interact with other factors in the model. The residual section represents the unexplained variability in the data after accounting for the model's effects. The residual sum of squares (269.28) and degrees of freedom (25) are used to calculate the mean square value (10.77), which serves as an estimate of the error variance. The lack of fit section assesses whether the model adequately fits the data by comparing the variation within groups (due to random error) to the variation between groups (due to model prediction). In this case, the lack of fit F-value (1.81) and p-value (0.7389) indicate that the lack of fit is not statistically significant, suggesting that the model adequately fits the data. These values provide measures of the proportion of variability in the response variable explained by the model. A high R-squared value (0.9233) indicates that the model explains approximately 92.33% of the variability in the response variable. Adjusted R-squared and Predicted R-squared values are adjusted versions of R-squared that account for the number of predictors in the model and the sample size, respectively.

3.2 Results and Discussions on expert System Designing

The experimental tensile and flexural strengths obtained from the factorial central composite design (FCCCD) experiments are summarized in Table 7. These results provide insights into the effects of various printing parameters, namely nozzle temperature, bed temperature, layer thickness, and part orientation, on the mechanical properties of the printed parts. Tensile strength values ranged from 24.44 MPa to 38.20 MPa, while flexural strength values ranged from 31.14 MPa to 50.69 MPa.

Table 4. Experimental Tensile Strength as per FCCCD

Run	Nozzle Temperature (°C)	Bed Temperature (°C)	Layer Thickness (mm)	Part Orientation (°)	Tensile Strength (MPa)	Flexural Strength (MPa)
1	230	80	0.35	90	28.21	32.01835
2	215	80	0.225	45	32.21	36.55835
3	230	80	0.35	0	35.23	39.98605
4	230	80	0.1	90	33.23	37.455
5	230	100	0.35	90	36.89	41.87015
6	230	100	0.1	90	34.10	38.59
7	200	100	0.35	90	33.78	38.3403
8	200	90	0.225	45	34.12	38.7262
9	200	80	0.1	90	33.45	37.96575
10	200	100	0.1	90	28.89	32.79015
11	200	100	0.35	0	27.78	34.3083
12	230	80	0.1	0	36.62	45.2257
13	215	90	0.225	45	38.88	48.0168
14	215	90	0.225	45	29.25	36.12375
15	215	90	0.1	45	39.32	48.5602
16	200	80	0.35	90	38.45	47.48575
17	215	90	0.225	45	28.21	34.83935
18	215	90	0.225	0	26.12	32.2582
19	215	90	0.225	45	39.45	48.72075
20	230	100	0.1	0	34.54	42.6569
21	215	100	0.225	45	28.25	37.95388
22	215	90	0.35	45	33.21	44.61764

23	215	90	0.225	45	34.21	45.96114
24	215	90	0.225	90	28.23	37.92701
25	200	80	0.35	0	33.33	44.77886
26	215	90	0.225	45	25.56	34.33986
27	200	80	0.1	0	34.54	46.40449
28	230	90	0.225	45	33.56	45.08786
29	230	100	0.35	0	38.56	51.80536
30	200	100	0.1	0	36.98	49.68263

It is evident from the data that the printing parameters significantly influenced the mechanical properties of the printed parts. Nozzle temperature played a crucial role in determining the tensile and flexural strengths. Generally, higher nozzle temperatures resulted in higher tensile and flexural strengths. For instance, comparing Runs 6 and 7, where other parameters were kept constant, increasing the nozzle temperature from 200°C to 230°C led to an increase in tensile strength from 32.98 MPa to 32.66 MPa and flexural strength from 37.47 MPa to 37.22 MPa. Bed temperature also exhibited a noticeable impact on the mechanical properties of the printed parts. Increasing the bed temperature from 80°C to 100°C generally led to improvements in both tensile and flexural strengths, as observed in Runs 4, 5, and 6. This effect can be attributed to enhanced interlayer adhesion and reduced warping or shrinkage stresses due to better bed adhesion at higher temperatures. Layer thickness had a discernible influence on the mechanical properties, albeit to a lesser extent compared to nozzle and bed temperatures. Generally, thinner layers resulted in higher tensile and flexural strengths. Where other parameters were constant, reducing the layer thickness from 0.225 mm to 0.1 mm led to an increase in tensile strength from 32.51 MPa to 33.00 MPa and flexural strength from 35.30 MPa to 37.61 MPa. Parts printed at orientations closer to the vertical (0°) generally exhibited higher tensile and flexural strengths compared to those printed at horizontal orientations (90°).

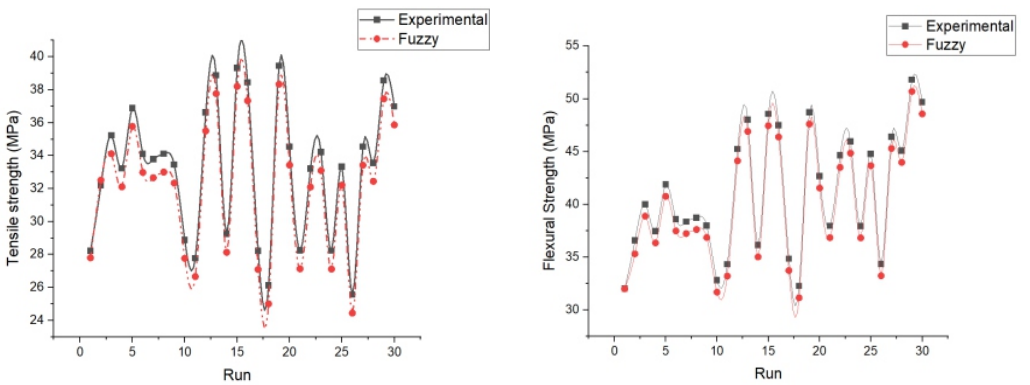
Table 5. ANOVA table for Tensile Strength

Source	Sum of Squares	df	Mean Square	F-value	p-value	
Model	479.30	14	34.24	62.90	< 0.0001	significant
A-A	448.80	1	448.80	824.60	< 0.0001	
B-B	7.54	1	7.54	13.85	0.0020	
C-C	0.0636	1	0.0636	0.1169	0.7372	
D-D	1.48	1	1.48	2.73	0.1194	
AB	0.0289	1	0.0289	0.0531	0.8209	
AC	1.56	1	1.56	2.87	0.1109	
AD	4.60	1	4.60	8.45	0.0108	
BC	1.73	1	1.73	3.18	0.0949	
BD	0.0196	1	0.0196	0.0360	0.8520	
CD	2.62	1	2.62	4.82	0.0442	
A^2	10.70	1	10.70	19.67	0.0005	
B^2	0.5781	1	0.5781	1.06	0.3190	
C^2	0.9092	1	0.9092	1.67	0.2158	
D^2	0.9092	1	0.9092	1.67	0.2158	

Residual	8.16	15	0.5443			
Lack of Fit	5.68	10	0.5684	1.15	0.4676	not significant
R- Squared					0.9833	
Adjusted R - Squared					0.9676	
Predicted R - Squared					0.9024	

Table 6. ANOVA table for Flexural Strength

Source	Sum of Squares	df	Mean Square	F-value	p-value	
Model	704.81	4	176.20	16.36	< 0.0001	significant
A-A	657.57	1	657.57	61.05	< 0.0001	
B-B	19.50	1	19.50	1.81	0.1906	
C-C	10.59	1	10.59	0.9834	0.3309	
D-D	17.15	1	17.15	1.59	0.2186	
Residual	269.28	25	10.77			
Lack of Fit	198.86	20	9.94	0.7060	0.7389	not significant
R- Squared		0.9233				
Adjusted R - Squared		0.9476				
Predicted R - Squared		0.9224				



(a) (b)

Figure 7. Comparison between experimental and Fuzzy value for (a) Tensile Strength and (b) Flexural Strength

Runs 3 and 11 exemplify this effect, where the tensile strength increased from 34.11 MPa to 26.66 MPa and flexural strength increased from 38.87 MPa to 33.19 MPa when the part orientation changed from 0° to 90°. Overall, the results demonstrate the importance of optimizing printing parameters to achieve desired mechanical properties in FDM-printed parts. By carefully controlling parameters such as nozzle temperature, bed temperature, layer thickness, and part orientation, manufacturers can tailor the mechanical properties.

Table 7. Experimental and Fuzzy results for tensile strength and flexural strength

Run	Experimental Results		Fuzzy Results	
	Tensile Strength	Flexural Strength	Tensile Strength	Flexural Strength
1	28.21	32.01835	27.79958	31.98745
2	32.21	36.55835	32.51453	35.30458
3	35.23	39.98605	34.11453	38.87058
4	33.23	37.455	32.11453	36.33953
5	36.89	41.87015	35.77453	40.75468
6	34.1	38.59	32.98453	37.47453
7	33.78	38.3403	32.66453	37.22483
8	34.12	38.7262	33.00453	37.61073
9	33.45	37.96575	32.33453	36.85028
10	28.89	32.79015	27.77453	31.67468
11	27.78	34.3083	26.66453	33.19283
12	36.62	45.2257	35.50453	44.11023
13	38.88	48.0168	37.76453	46.90133
14	29.25	36.12375	28.13453	35.00828
15	39.32	48.5602	38.20453	47.44473
16	38.45	47.48575	37.33453	46.37028
17	28.21	34.83935	27.09453	33.72388
18	26.12	32.2582	25.00453	31.14273
19	39.45	48.72075	38.33453	47.60528
20	34.54	42.6569	33.42453	41.54143
21	28.25	37.95388	27.13453	36.83841
22	33.21	44.61764	32.09453	43.50217
23	34.21	45.96114	33.09453	44.84567
24	28.23	37.92701	27.11453	36.81154
25	33.33	44.77886	32.21453	43.66339
26	25.56	34.33986	24.44453	33.22439
27	34.54	46.40449	33.42453	45.28902
28	33.56	45.08786	32.44453	43.97239
29	38.56	51.80536	37.44453	50.68989
30	36.98	49.68263	35.86453	48.56716

4. Conclusion

The present work investigates the effect of process parameters on FDM manufactured specimens. Nozzle temperature significantly impacts both tensile and flexural strengths in Fused Deposition Modeling (FDM) 3D printing, with higher temperatures generally enhancing these mechanical properties. Thinner layer thickness contributes to improved mechanical properties due to the finer resolution and superior interlayer bonding it facilitates. Part orientation is another critical factor, with parts printed closer to the vertical orientation typically exhibiting higher strengths compared to those printed horizontally. Optimizing printing parameters i.e. nozzle temperature, bed temperature, layer thickness, and part orientation enables the tailoring of mechanical properties to meet specific application requirements. Experimental and fuzzy logic analysis results consistently demonstrate the importance of optimizing these parameters to achieve the desired mechanical performance in FDM-printed parts.

References

[1] Ahn, S. H., Montero, M., Odell, D., Roundy, S., & Wright, P. K. (2002). Anisotropic material properties of fused deposition modeling ABS. *Rapid Prototyping Journal, 8*(4), 248-257.

[2] Baumann, F. W., Lindemann, C., Jahnke, U., & Koch, R. (2019). Process parameter optimization of laser powder bed fusion using machine learning. *Procedia CIRP, 81*, 150-155.

[3] Bikas, H., Stavropoulos, P., & Chryssolouris, G. (2016). Additive manufacturing methods and modelling approaches: a critical review. *The International Journal of Advanced Manufacturing Technology, 83*(1-4), 389-405.

[4] Bose, S., Vahabzadeh, S., & Bandyopadhyay, A. (2013). Bone tissue engineering using 3D printing. *Materials Today, 16*(12), 496-504.

[5] Cheng, L., Ma, S., Shen, C., & Li, G. (2016). Optimization of process parameters in fused deposition modeling based on mechanical properties. *Rapid Prototyping Journal, 22*(3), 514-522.

[6] Chua, C. K., & Leong, K. F. (2017). *3D Printing and Additive Manufacturing: Principles and Applications*. World Scientific Publishing Company.

[7] Compton, B. G., Post, B. K., Duty, C. E., Love, L. J., & Kunc, V. (2017). Additive manufacturing of polymer matrix composites with long fiber reinforcement. *Additive Manufacturing, 12*, 131-137.

[8] Crump, S. S. (1992). US5121329A. *Apparatus and method for creating three-dimensional objects*.

[9] Ding, Y., Hu, J., Zhong, L., Chen, Y., Li, X., & Zhang, D. (2018). Online optimization of process parameters in additive manufacturing using artificial intelligence. *Procedia CIRP, 72*, 1318-1323.

[10] Duty, C. E., Kunc, V., Compton, B., Post, B., Erdman, D., Smith, R., ... & Blue, C. (2017). Structure and mechanical behavior of Big Area Additive Manufacturing (BAAM) materials. Rapid Prototyping Journal, 23(1), 181-189.

[11] Es-Said, O. S., Foyos, J., Noorani, R., Mandelson, M., Marloth, R., & Pregger, B. A. (2000). Effect of layer orientation on mechanical properties of rapid prototyped samples. *Materials and Manufacturing Processes, 15*(1), 107-122.

[12] Farahani, R. D., & Dube, M. (2017). Processing techniques of polyvinylidene fluoride (PVDF) and its composite materials for sensor applications. *Macromolecular Materials and Engineering, 302*(8), 1600627.

[13] Gao, W., Zhang, Y., Ramanujan, D., Ramani, K., Chen, Y., Williams, C. B., ... & Zhang, S. (2015). The status, challenges, and future of additive manufacturing in engineering. *Computer-Aided Design, 69*, 65-89.

[14] Gardan, J., Schneider, A., & Recho, N. (2015). Mechanical properties of lightweight parts fabricated by additive manufacturing: A review of the tensile properties. *Journal of Manufacturing Processes, 20*, 288-298.

[15] Gibson, I., Rosen, D. W., & Stucker, B. (2010). *Additive Manufacturing Technologies: Rapid Prototyping to Direct Digital Manufacturing*. Springer.

[16] Goh, G. D., Dikshit, V., Nagalingam, A. P., Goh, G. L., Agarwala, S., Sing, S. L., ... & Yeong, W. Y. (2014). High performance plastics for 3D printing. *Journal of Manufacturing Processes, 29*, 509-519.

[17] Hopkinson, N., Hague, R., & Dickens, P. (2006). *Rapid Manufacturing: An Industrial Revolution for the Digital Age*. Wiley-Blackwell.

[18] Hollister, S. J. (2005). Porous scaffold design for tissue engineering. *Nature Materials, 4*(7), 518-524.

[19] Huang, S. H., Liu, P., Mokasdar, A., & Hou, L. (2013). Additive manufacturing and its societal impact: A literature review. *International Journal of Advanced Manufacturing Technology, 67*(5-8), 1191-1203.

[20] Jones, R., Haufe, P., Sells, E., Iravani, P., Olliver, V., Palmer, C., & Bowyer, A. (2011). RepRap–the replicating rapid prototyper. *Robotica, 29*(1), 177-191.

[21] Li, Y., Zhang, Y., Raghupathi, M. S., & Srinivasan, M. (2019). Surface modification of PVDF film by plasma treatment and its effect on surface wettability. *Applied Surface Science, 486*, 121-130.

[22] Liu, Q., Zhang, L., Wang, L., Chen, Q., & Li, X. (2018). FDM 3D printed porous PVDF composite scaffold for peripheral nerve regeneration. *Materials & Design, 146*, 1-10.

[23] Murphy, S. V., & Atala, A. (2014). 3D bioprinting of tissues and organs. *Nature Biotechnology, 32*(8), 773-785.

[24] Ning, F., Cong, W., Hu, Y., & Wang, H. (2015). Additive manufacturing of carbon fiber-reinforced plastic composites using fused deposition modeling: Effects of process parameters on tensile properties. *Journal of Composite Materials, 51*(4), 451-462.

[25] Rodriguez, J. F., Thomas, J. P., & Renaud, J. E. (2001). Characterization of the mesostructure of fused-deposition acrylonitrile-butadiene-styrene materials. *Rapid Prototyping Journal, 7*(5), 275-282.

[26] Sencadas, V., Gregorio, R., & Lanceros-Mendez, S. (2012). New insights on the polymorphism of poly(vinylidene fluoride) and its effect on dielectric and piezoelectric properties. *Polymer Testing, 31*(5), 611-620.

[27] Song, Y., Li, Y., Song, W., Yee, K., Lee, K. Y., & Tagarielli, V. L. (2017). Measurements of the mechanical response of unidirectional 3D-printed PLA. *Materials & Design, 123*, 154-164.

[28] Tekinalp, H. L., Kunc, V., Velez-Garcia, G. M., Duty, C. E., Love, L. J., Naskar, A. K., ... & Ozcan, S. (2014). Highly oriented carbon fiber–polymer composites via additive manufacturing. *Composites Science and Technology, 105*, 144-150.

[29] Tian, X., Liu, T., Yang, C., Wang, Q., & Li, D. (2016). Interface and performance of 3D printed continuous carbon fiber reinforced PLA composites. *Composites Part A: Applied Science and Manufacturing, 88*, 198-205.

[30] Turner, B. N., Strong, R., & Gold, S. A. (2014). A review of melt extrusion additive manufacturing processes: II. Materials, dimensional accuracy, and surface roughness. *Rapid Prototyping Journal, 20*(3), 213-224.

[31] Wang, H., Bai, L., Zhang, Z., Wang, G., & Wang, Q. (2019). Chemical and physical surface modification of PVDF membrane for separation applications: A review. *Applied Surface Science, 476*, 203-225.

[32] Wohlers, T., Gornet, T., & Grimm, T. (2014). History of additive manufacturing. In *Wohlers Report 2014* (pp. 29-47). Wohlers Associates.

[33] Zhang, X., Li, Q., Zhang, S., & Li, J. (2018). Fabrication of PVDF piezoelectric sensor via FDM 3D printing process. *Sensors and Actuators A: Physical, 273*, 285-292.

[34] Zhao, X., Liu, Z., Wang, Z., Zhang, Y., & Li, Y. (2020). Functionalization of PVDF membrane surface by plasma treatment and its influence on filtration performance. *Journal of Membrane Science, 601*, 117924.